J Mol Model (2010) 16:659–668
DOI 10.1007/s00894-009-0623-x

ORIGINAL PAPER

DFT study of linear and nonlinear optical properties of donor-acceptor substituted stilbenes, azobenzenes and benzilideneanilines

Przemysław Krawczyk

Received: 21 June 2009 / Accepted: 4 November 2009 / Published online: 4 December 2009

Abstract A theoretical analysis of the linear and nonlinear optical properties of six push–pull π-conjugated molecules with stilbene, azobenzene and benzilideneaniline as a backbone is presented. The photophysical properties of the investigated systems were determined by using response functions combined with density functional theory (DFT). Several different exchange-correlation potentials were applied in order to determine parameters describing the one- and two-photon spectra of the studied molecules. In particular, the recently proposed Coulomb-attenuated model (CAM-B3LYP) was used to describe charge-transfer (CT) excited states. In order to compare theoretical predictions with available experimental data, calculations with inclusion of solvent effects were performed. The BLYP and the CAM-B3LYP functionals were found to yield values of two-photon absorption (TPA) probabilities closer to experimental values than the B3LYP functional or the HF wavefunction. Moreover, molecular static hyperpolarisabilities were determined using both DFT and second-order Møller-Plesset perturbation (MP2) theory. Likewise, the CAM-B3LYP functional was found to outperform other applied exchange-correlation potentials in determining first hyperpolarisability (β). Moreover, it was confirmed on a purely theoretical basis that the presence of a –C=C– bridge between the phenyl rings leads to a much larger nonlinear optical response in comparison with a –N=N– bridge.

P. Krawczyk (✉)
Department of Physical Chemistry, Collegium Medicum,
Nicolaus Copernicus University,
Kurpińskiego 5,
85-950 Bydgoszcz, Poland
e-mail: przemekk@cm.umk.pl

Keywords Photoswitching · Density functional theory · CAM-B3LYP functional · Azobenzenes · Stilbenes · Electronic excited states

Introduction

The nonlinear optical (NLO) properties of noncentrosymmetrical π-conjugated organic molecules, containing electron-donating (D) and electron-accepting (A) substituents, have been the subject of intense research during recent years [1–7].

One of the major problems in designing new NLO polymeric materials is the choice of chromophore [8, 9]. Chromophores with potential application in photonics should possess large hyperpolarisability values which, to some extent, can be achieved by combining a π-conjugated bridge with D/A substituents. This type of molecule is commonly known as a push–pull system. The presence of D/A substituents leads to nonsymmetrical electron density distribution in the ground state. On the other hand, a π-conjugated bridge facilitates electron redistribution in an external electric field. Thus, the NLO response of organic π-conjugated molecules is determined to a large extent by their size. Yet another important factor determining the macroscopic NLO response of a material is the ability of chromophores to orient in the presence of an external electric field [10].

Theoretical investigations of electronic structure and the NLO properties of molecules (molecular hyperpolarisabilities, two-photon absorptivities) can allow structure-property relationships to be established. Nowadays, it is widely accepted that the value of first hyperpolarisability can be modulated substantially by appropriate choice of the strength of D/A substituents and the length of the

π-conjugated bridge. For a given pair of D/A substituents, there is an optimal length of π-conjugated bridge maximizing β [11]. As components of model studies, a wide group of D/A substituted benzenes, stilbenes and azoaromatic compounds have been investigated to date [12–17]. As a result, it has been found that push–pull systems exhibit (in comparison with similar unsubstituted species) large values of molecular hyperpolarisabilities and two-photon absorption (TPA) cross sections which, in turn, are connected with significant polarity differences between the low-lying excited state and the ground state [18–25]. Application of the two-state model (TSM) proposed by Oudar and Chemla [26], allows us to choose D/A substituents in such a way as to maximise the first hyperpolarisability. Organic materials and organic-inorganic hybrids of large hyperpolarisabilities have been applied successfully to optical data storage [27] and photoswitching [28].

Density functional theory (DFT) is nowadays commonly used to describe the excited states of molecules of different types [29–31]. Some of the most frequently used functionals for this purpose are B3LYP [32] and PBE0 [33]. Despite their relatively satisfactory performance in determination of the spectra of numerous groups of organic molecules, they are known to poorly predict excitation energies of the charge-transfer and the Rydberg states [34]. In order to improve the predictions of traditional functionals, long-range corrected schemes have been proposed recently [34, 35]. One such scheme is the CAM-B3LYP functional, which introduces the Hartree-Fock (HF) exchange energy at large distances. This functional was proven to yield much better results for (hyper)polarisabilities as well as excitation energies to the charge-transfer and the Rydberg states [36–38]. A less general approach, namely the LC-BLYP (long-range corrected BLYP), was also found to predict NLO properties quite satisfactorily for organic compounds like azobenzenes or stilbenes [39]. The aim of the present study was to analyse, on a purely theoretical basis, the relationship between the electronic structure and the NLO properties of model D/A substituted azobenzenes, benzilideneanilines and stilbenes (see Fig. 1). TPA cross-sections of these molecules have already been determined experimentally by Antonov et al. [24, 25]. An important part of the study was also the comparison of various theoretical models (DFT, many-body perturbation theory, coupled cluster approach) used to determine spectra, molecular hyperpolarisabilities and two-photon absorptivities.

Computational details

The geometry of molecules in their ground state was optimised using the hybrid exchange-correlation B3LYP functional with 6–311++G(d,p) basis set. In all cases, the

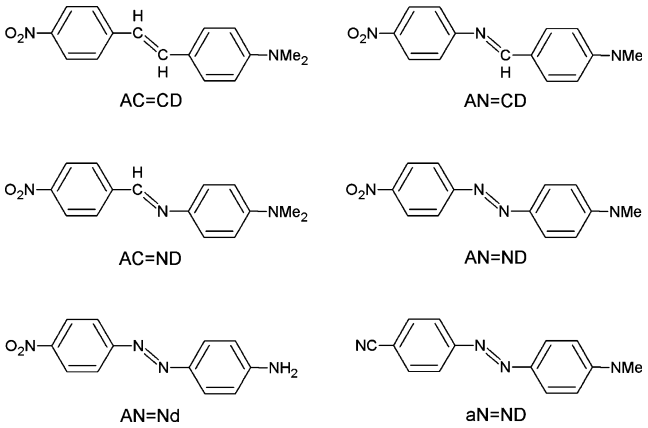

Fig. 1 Chemical structures of the investigated noncentrosymmetric molecules

Hessian was computed in order to confirm that the stationary points correspond to minima on the potential energy surface. Solvent effects were taken into account with the aid of the polarisable continuum model IEF-PCM [in all cases, geometry optimisation in a given solvent was performed using the B3LYP functional and the 6–311+G(d, p) basis set] and the self-consistent reaction field (SCRF) method was used for all CAM-B3LYP computations with inclusion of solvent effects.

Spectroscopic parameters characterising one-photon excitation spectra (including excited state dipole moments) were determined using time-dependent density functional theory (TD-DFT) using the Gaussian 03 [40], Dalton 2.0 [41] and GAMESS US [42] packages. Excitation energies and dipole moments were also computed using the coupled-cluster CC2 model [43–45] of the TURBOMOLE package.

In the case of absorption of two-photons of the same energy in isotropic media, the averaged TPA cross section is given by [46]:

$$\left\langle \delta^{OF} \right\rangle = \frac{1}{15} \sum_{ij} \left[S_{ii}^{OF} \left(S_{jj}^{OF} \right)^{*} + 2 S_{ij}^{OF} \left(S_{ij}^{OF} \right)^{*} \right] \tag{1}$$

In the above equation, S_{ij}^{OF} is the second-order transition moment given by:

$$S_{ij}^{OF}(\zeta_1, \zeta_2) = \frac{1}{h} \sum_{K} \left[\frac{\left\langle 0 \left| \zeta_1 \cdot \bar{\mu}_i \right| K \right\rangle \left\langle K \left| \zeta_2 \cdot \bar{\mu}_j \right| F \right\rangle}{\omega_K - \omega_1} + \frac{\left\langle 0 \left| \zeta_2 \cdot \bar{\mu}_i \right| K \right\rangle \left\langle K \left| \zeta_1 \cdot \bar{\mu}_j \right| F \right\rangle}{\omega_K - \omega_2} \right] \tag{2}$$

where $\hbar\omega_1 + \hbar\omega_2$ should satisfy the resonance condition and $\left\langle 0 \left| \zeta_1 \cdot \bar{\mu}_i \right| K \right\rangle$ stand for the transition moment between electronic states $|0\rangle$ and $|K\rangle$, respectively. ζ is the vector defining polarisation of photons. Here, the photons are assumed to be polarised linearly. All calculations of TPA cross sections (as single residues of quadratic response functions) were performed using the DALTON 2.0 program.

In order to compute molecular first hyperpolarisability (β) we used the Taylor expansion of the total energy (E) with respect to electric field (F):

$$E(F) = E(0) - \mu_i F_i - \frac{1}{2!}\alpha_{ij}F_iF_j - \frac{1}{3!}\beta_{ijk}F_iF_jF_k - \frac{1}{4!}\gamma_{ijkl}F_iF_jF_kF_l - \ldots \quad (3)$$

where $E(0)$ is the energy of a molecule without the presence of a field. All elements of β tensor were determined by numerical differentiation of the total energy given by Eq. 3 with respect to a field. All computations employed an electric field of 0.001 a.u. strength, but in several cases the stability of derivatives was checked by applying the Romberg differentiation procedure. The computations of first hyperpolarisability, using second-order Møller-Plesset perturbation (MP2) and HF methods as well using the BLYP and the B3LYP functionals, were performed using the GAMESS program [42] while the DALTON 2.0 program [41] was used for the CAM-B3LYP calculations.

In the LC method, the two-electron operator $1/r_{12}$ is separated into short-range and the long-range parts by using the standard error function [39]:

$$\frac{1}{r_{12}} = \frac{1 - erf(\mu r_{12})}{r_{12}} + \frac{erf(\mu r_{12})}{r_{12}} \quad (4)$$

where μ is a damping parameter. The exchange functional is then obtained by using the long-range part in the HF exchange expression, while the short-range part modifies a conventional DFT exchange potential. In the CAM procedure, the form of Eq. 4 is generalised by using two extra parameters α and β [36–38]:

$$\frac{1}{r_{12}} = \frac{1 - [\alpha + \beta\, erf(\mu r_{12})]}{r_{12}} + \frac{\alpha + \beta\, erf(\mu r_{12})}{r_{12}} \quad (5)$$

where α and β are dimensionless parameters satisfying the following conditions $0 \le \alpha + \beta \le 1$, $0 \le \alpha \le 1$, and $0 \le \beta \le 1$. This allows an amount α (fraction of HF exchange, for short-range interactions) of exact orbital exchange to remain as $r_{12} \to 0$,and an amount ($\alpha + \beta$; fraction for long-range) to remain as $r_{12} \to \infty$. Within this formalism, LC-DFT corresponds to α=0.0 and β=1.0, whereas B3LYP uses α=0.2 and β=0.0. For CAM-B3LYP, α=0.19, β=0.46 and μ=0.33 were used in all calculations.

Results and discussion

One-photon absorption

As mentioned in the Introduction, the systems studied belong to the D–π–A class of compounds. The electronic spectra of these compounds exhibit very intense bands associated with the so-called intramolecular charge-transfer [47, 48]. The extent of this transfer depends crucially on the strength of the D/A substituents and the nature of the π-bridge, and is reflected in the intensity and location of the band in one-photon spectra.

Table 1 presents the results of DFT calculations (with the aid of four different functionals) of spectroscopic parameters characterising the lowest-lying singlet excited states. It can be seen that the charge-transfer state is the first excited singlet state in all molecules except azobenzene derivatives [20]. For these systems, both B3LYP and PBE0 predict the transition to the lowest-lying state to be more intense than to the second singlet state. The excitations to the two lowest-lying singlet states, of π–π* character, involve mainly HOMO (highest occupied molecular orbital) →LUMO (lowest unoccupied molecular orbital) and HOMO→LUMO+1 transitions. Table 1 also contains the results of calculations using CAM-B3LYP and LC-BLYP functionals. For azobenze derivatives, the excitation of the lowest-energy is of n–π* character while intense charge-transfer excitation is observed for the second excited singlet state [49, 50].

The energy difference (ΔE) between the excitation energies calculated for CT states using the LC-BLYP functional for AN=ND and AN=Nd is 18 nm; for AN=ND and aN=ND is 7 nm and for aN=ND and AN=Nd is 11 nm. The value of transition energy to the CT excited state changes as the strength of the D/A substituents decreases. Similar results were obtained for the other functionals employed. It is now widely recognised that increasing the strength of D/A substituents leads to a decrease in transition energy to the low-lying charge-transfer state. For a given pair of D/A substituents, the largest excitation energy is observed for AC=CD, while the lowest excitation energy to the CT state is found for AC=ND. In the case of AC=ND and AN=CD compounds, we see a significant difference in excitation energy computed at the CAM-B3LYP/6–311++G(d,p) and LC-BLYP/6–311++G(d,p) levels of theory.

In order to asses the reliability of TD-DFT excitation energy results for isolated systems, response calculations using the CC2 method were also performed (see Table 1). Judging by the values of excitation energies corresponding to the lowest π–π* transition, the CAM-B3LYP model outperforms the other employed functionals. The average difference between CC2 and CAM-B3LYP excitation energies does not exceed 14 nm. Similarly good performance of this functional in computing spectra of π-conjugated organic molecules has also been reported by other authors [34, 51–55]. As can be seen in Table 2, both PBE0 and B3LYP tend to underestimate excitation energy in the gas phase. The discrepancy is even more pronounced

Table 1 Absorption maxima (λ_{max}) and oscillator strengths (f) for the tested molecules in gas phase calculated using the 6–311++G(d,p) basis set for the geometries optimised at B3LYP/6–311++D(d,p) level of theory

		B3LYP		PBE0		CAM-B3LYP		LC-BLYP		CC2	
		λ_{max}	f	λ_{max}	f	λ_{max}	f	λ_{max}	f	λ_{max}	f
AC=CD	2^1A	475	0.77	447	0.87	379	1.23	349	1.32	381	1.29
	3^1A	334	0.36	319	0.32	319	0.00	275	0.04	321	0.05
	4^1A	334	0.04	327	0.00	284	0.01	263	0.01	301	0.02
AN=CD	2^1A	421	0.55	395	0.69	338	1.19	321	0.68	347	1.28
	3^1A	340	0.42	327	0.20	318	0.00	321	0.53	318	0.00
	4^1A	330	0.04	322	0.12	288	0.02	282	0.10	296	0.01
AC=ND	2^1A	517	0.53	484	0.59	389	0.82	354	0.85	403	0.85
	3^1A	350	0.16	334	0.07	320	0.00	288	0.27	321	0.00
	4^1A	335	0.00	328	0.00	295	0.12	273	0.05	–	–
AN=ND	2^1A	511	0.00	499	0.00	460	0.00	457	0.00	449	0.00
	3^1A	461	0.88	440	0.97	389	1.69	368	1.19	419	1.16
	4^1A	345	0.23	326	0.16	321	0.00	270	0.03	321	0.00
AN=Nd	2^1A	509	0.00	498	0.00	460	0.00	457	0.00	448	0.00
	3^1A	428	0.84	409	0.92	369	1.08	350	1.08	375	1.09
	4^1A	338	0.00	330	0.00	321	0.00	267	0.01	321	0.00
aN=ND	2^1A	491	0.00	484	0.00	454	0.00	452	0.00	443	0.00
	3^1A	422	1.07	410	1.11	377	1.19	361	1.20	409	1.16
	4^1A	306	0.02	296	0.09	276	0.02	269	0.03	285	0.02

Table 2 Excitation energies (ΔE) and oscillator strengths (f) calculated at the time-dependent density functional theory (TD-DFT)/6–311++G(d,p) level of theory with the inclusion of solvent effects. The values of excitation energies to the charge transfer state computed using CAM-B3LYP functional are given in parentheses. *THF* Tetrahydrofuran, *DMSO* dimethylsulphoxide

	Experimental (DMSO)		Heptane				THF				DMSO			
			B3LYP		PBE0		B3LYP		PBE0		B3LYP		PBE0	
			λ_{max}	f	λ_{max}	f	λ_{max}	f	λ_{max}	f	λ_{max}	f	λ_{max}	f
AC=CD	452 (398)	2^1A	527	0.90	494	0.10	574	0.91	536	0.10	595	0.94	555	1.02
		3^1A	348	0.51	332	0.43	363	0.56	344	0.52	369	0.55	349	0.53
		4^1A	333	0.00	327	0.00	333	0.00	327	0.00	344	0.02	327	0.00
AN=CD	416 (352)	2^1A	466	0.59	432	0.73	515	0.54	473	0.66	535	0.54	489	0.66
		3^1A	353	0.62	337	0.50	366	0.73	349	0.66	371	0.77	353	0.71
		4^1A	330	0.03	323	0.03	328	0.14	324	0.03	328	0.00	324	0.09
AC=ND	460 (408)	2^1A	569	0.62	528	0.69	608	0.67	561	0.73	629	0.68	578	0.74
		3^1A	363	0.25	345	0.17	372	0.35	353	0.27	376	0.37	357	0.30
		4^1A	334	0.00	328	0.01	341	0.02	327	0.00	333	0.01	327	0.00
AN=ND	501 (408)	2^1A	518	0.02	504	0.01	521	0.03	503	0.31	526	0.00	508	0.03
		3^1A	505	0.99	480	1.10	540	0.98	513	0.80	557	1.04	525	1.12
		4^1A	363	0.26	343	0.19	380	0.34	359	0.25	386	0.35	366	0.26
AN=Nd	478 (381)	2^1A	515	0.01	502	0.01	523	0.00	506	0.00	523	0.13	510	0.38
		3^1A	476	0.97	453	1.06	513	0.98	485	1.08	534	0.89	500	0.74
		4^1A	335	0.00	329	0.00	353	0.00	331	0.00	333	0.00	327	0.00
aN=ND	470 (385)	2^1A	492	0.00	485	0.00	489	0.00	483	0.00	488	0.01	482	0.00
		3^1A	450	1.23	438	1.27	463	1.27	450	1.30	471	1.29	457	1.33
		4^1A	310	0.02	299	0.01	314	0.03	303	0.01	316	0.03	304	0.02

Table 3 Values of dipole moments calculated for the ground and two lowest-lying singlet electronic excited states. TD-DFT calculations were performed using the 6–311++G(d,p) basis set while CC2 computations were performed using cc-pVDZ. Experimental values are taken from [18, 19]. All values are given in [D]

		Experimental DMSO	Gas phase			Heptane		THF		DMSO	
			CC2	B3LYP	PBE0	B3LYP	PBE0	B3LYP	PBE0	B3LYP	PBE0
AC=CD	1^1A	7.4	9.5	11.2	11.0	12.9	12.6	15.1	14.7	16.1	15.5
	2^1A	26.0	25.7	26.9	26.5	30.3	30.1	33.7	34.1	35.0	35.6
	3^1A	–	6.3	7.4	7.4	8.7	8.5	15.8	9.9	19.0	10.3
AN=CD	1^1A	8.6	10.5	11.9	11.7	13.5	13.3	15.5	15.2	16.2	15.9
	2^1A	23.9	22.4	32.3	30.4	36.9	35.3	42.2	41.1	44.0	43.1
	3^1A	–	7.8	9.9	7.6	10.1	11.4	11.8	11.7	10.8	6.0
AC=ND	1^1A	6.9	8.6	9.9	9.8	11.3	11.0	13.1	12.7	13.7	13.2
	2^1A	23.0	26.1	27.2	26.9	30.8	30.8	34.4	34.9	35.8	36.5
	3^1A	–	5.4	6.4	6.1	7.1	7.0	14.8	8.2	15.0	8.5
AN=ND	1^1A	8.0	10.4	11.8	11.6	13.5	13.3	16.0	15.6	17.0	16.5
	2^1A	–	11.5	14.5	13.6	17.2	16.2	20.7	18.8	23.5	20.3
	3^1A	25.0	23.4	24.0	23.1	27.7	26.5	32.7	31.7	33.1	33.2
AN=Nd	1^1A	–	8.6	10.1	10.0	12.5	12.3	15.2	14.8	16.7	16.3
	2^1A	–	9.7	12.8	12.0	16.4	15.1	20.6	18.6	22.4	20.1
	3^1A	–	19.6	21.3	20.3	25.7	24.7	30.6	29.7	32.9	32.1
aN–ND	1^1A	–	10.4	10.9	10.8	12.4	12.3	14.2	14.0	14.9	14.7
	2^1A	–	10.9	11.9	11.6	13.5	13.1	15.4	14.9	16.2	15.5
	3^1A	–	22.4	17.4	17.5	19.8	20.0	22.5	22.6	23.4	23.6

if we compare experimental excitation energies with the results of calculations in dimethylsulphoxide (DMSO). The difference can even exceed 140 nm for AC=CD at the B3LYP/6–311++G** level of theory (see Table 2).

The influence of the solvent on the one-photon excitation energies is presented in Table 2. Experimental band maxima are also given for comparison [24]. In all cases considered, a positive solvatochromism was observed. It should be underscored that in the case of DMSO the difference $\lambda_{\max}^{DMSO} - \lambda_{\max}^{gas\,phase}$ is 100% larger than with heptane. If we consider different D/A substituents, we see that the batochromic shift is almost two times larger in the case of AN=Nd than for aN=ND. The values of $\lambda_{\max}^{solvent} - \lambda_{\max}^{gas\,phase}$ calculated with PBE0 functional for heptane, tetrahydrofuran (THF) and DMSO are 44, 76 and 91 nm for AN=Nd, respectively. Thus, we see that the presence of a weak acceptor and strong donor strongly diminishes excitation energy to the charge-transfer state, and the lowest excitation energy to the CT state is found for stilbene derivatives.

Comparing the experimentally determined absorption band maxima with theoretical excitation energies computed using the PBE0 functional, we see that the overall agreement is quite satisfactory and the differences do

Table 4 Dipole moment differences (Δμ) between the low-lying excited states and the ground state. All values are given in [D]. Experimental values are taken from [55]

	Experimental (benzene)	Gas phase				Heptane		THF		DMSO	
		CAM-B3LYP	CC2	B3LYP	PBE0	B3LYP	PBE0	B3LYP	PBE0	B3LYP	PBE0
AC=CD	18.9	11.9	16.2	15.7	15.5	17.4	17.5	18.6	19.4	18.9	20.1
AN=CD	14.8	8.6	11.9	20.4	18.7	23.4	22.0	26.7	25.9	27.8	27.2
AC=ND	16.4	13.7	17.5	17.3	17.1	19.5	19.8	21.3	22.2	22.1	23.3
AN=ND	17	8.4	13.0	12.2	11.5	14.2	13.2	16.7	16.1	16.1	16.7
AN=Nd	–	7.2	11.0	11.2	10.3	13.2	12.4	15.4	14.9	16.2	15.8
aN=ND	–	6.3	12.0	6.5	6.7	7.4	7.7	8.3	8.6	8.5	8.9

Table 5 Values of two-photon absorption (TPA) cross-section ($\delta^{OF} \times 10^{-3}$) calculated using Eq. 1 using 6–311++G(d,p) basis set. All values are in atomic units

$<\delta^{OF}>$	Gas phase				DMSO			
	HF	B3LYP	BLYP	CAM-B3LYP	HF	B3LYP	BLYP	CAM-B3LYP
AC=CD	10.8	104.7	112.8	49.7	–	182.9	183.8	88.9
AN=CD	4.2	63.1	90.7	19.4	8.7	115.0	172.1	38.9
AC=ND	12.8	123.4	133.5	50.8	18.5	218.1	214.2	89.0
AN=ND	9.8	62.4	78.6	29.6	23.4	119.9	141.1	55.6
AN=Nd	5.5	38.6	54.3	16.8	9.9	64.2	85.9	27.9
aN=ND	5.9	19.1	19.1	15.3	8.2	27.2	31.9	21.5

not exceed 25 nm for azobenzene derivatives; for the remaining molecules, the differences are quite large and might exceed even 100 nm. Perhaps this discrepancy has its roots in incorrect asymptotics of traditional functionals.

Polarity of low-lying excited states

The results of experimental and calculated excited state dipole moments (μ) for the systems investigated are presented in Table 3. It can be seen that both B3LYP and PBE0 predict similar values of dipole moments for the studied molecules—the difference does not exceed 1 D and 1.5 D for the ground and the CT state, respectively. In order to check the validity of the excited state dipole moments, results of CC2 calculations were used as a reference. Both employed functionals tend to overestimate the excited state dipole moments in comparison to the CC2 method although the difference in most cases does not exceed 4 D. Only for AC=ND was the discrepancy quite large, reaching 10 D. Interestingly, ordering of the compounds according to the magnitude of the dipole moment in the ground state is quite different for the solvents than for the gas phase. As far as excited state dipole moments are concerned, we see that B3LYP and PBE0 functionals give values of Δμ much closer to those determined at the CC2 level of theory. The average difference between the CAM-B3LYP and CC2 dipole moment differences is 4.3 D, while the difference for the B3LYP functional is only 2.6 D. It is also worthwhile analysing how the polarity of the excited state depends on the nature of the π-bridge present in the molecule, see Table 4. For this purpose four molecules containing the same pair of D/A substituents, namely NO_2 and NMe_2 groups, were examined. Analysis of the polarity of the CT excited state for these four isolated systems using the CAM-B3LYP and CC2 methods gives the following order:

$$\Delta\mu_{g-CT}\mathrm{AC} = \mathrm{ND} > \Delta\mu_{g-CT}\mathrm{AC} = \mathrm{CD} > \Delta\mu_{g-CT}\mathrm{AN} = \mathrm{ND} > \Delta\mu_{g-CT}\mathrm{AN} = \mathrm{CD},$$

while in the case of B3LYP and PBE0 functionals one obtains a different sequence (which is the same in both the gas phase as well as in DMSO):

$$\Delta\mu_{g-CT}\mathrm{AN} = \mathrm{CD} > \Delta\mu_{g-CT}\mathrm{AC} = \mathrm{ND} > \Delta\mu_{g-CT}\mathrm{AC} = \mathrm{CD} > \Delta\mu_{g-CT}\mathrm{AN} = \mathrm{ND}$$

The ordering of dipole moment differences (Δμ) resulting from measurements performed in benzene [56] is:

$$\Delta\mu_{g-CT}\mathrm{AC} = \mathrm{CD} > \Delta\mu_{g-CT}\mathrm{AN} = \mathrm{ND} > \Delta\mu_{g-CT}\mathrm{AC} = \mathrm{ND} > \Delta\mu_{g-CT}\mathrm{AN} = \mathrm{CD}$$

Comparison between experimental values and the theory presented here is difficult as both Tables 3 and 4 present vertical dipole moment differences.

Obviously, Δμ is also determined by the nature of the D/A substituents. Considering three different pairs of substituents we find the following relationship for the dipole moment difference between the ground and the excited charge-transfer state ($\Delta\mu_{g-CT}$):

$$\Delta\mu_{g-CT}\mathrm{AN} = \mathrm{ND} > \Delta\mu_{g-CT}\mathrm{AN} = \mathrm{Nd} > \Delta\mu_{g-CT}\mathrm{aN} = \mathrm{ND}$$

Table 6 Comparison of exact (second column) and approximate (third column, see Eq. 6) TPA cross-section $<\delta^{OF}>$ calculated for molecules in vacuo at the CAM-B3LYP/6–311++G(d,p) level of theory. The final state is the lowest-lying charge-transfer state. All values are in atomic units

	$<\delta^{OF}>$	$\left\langle \delta^{ZZ}_{gCT} \right\rangle TSM$	$\frac{\left\langle \delta^{ZZ}_{gCT} \right\rangle}{\left\langle \delta^{0F} \right\rangle}$
AC=CD	49,662	72,681	1.5
AN=CD	19,450	26,416	1.4
AC=ND	50,866	66,939	1.3
AN=ND	29,642	38,532	1.3
AN=Nd	16,844	21,433	1.3
aN=ND	15,257	19,732	1.3

Table 7 Comparison of exact (second column) and approximate (third column, see Eq. 2) second-order transition moment (S_{zz}) calculated for molecules in vacuo at the CAM-B3LYP/6–311++G(d, p) level of theory. The final state is the lowest-lying charge-transfer state. All values are in atomic units

	S_{zz}^{gCT} TSM	S_{zz}^{gCT}
AC=CD	−602.8	499.8
AN=CD	−363.4	−313.2
AC=ND	578.5	489.5
AN=ND	438.9	−386.7
AN=Nd	327.4	289.8
aN=ND	−314.1	277.7

which holds for all but one case. The presence of an environment, even a solvent of low polarity such as heptane, results in an increase in polarity of the charge-transfer state. Although Δμ increases with the polarity of the solvent, ΔΔμ decreases slightly on passing from gas-phase to heptane, from heptane to THF and from THF to DMSO. Considering the differences in the π-bridge, we find the largest value of $\Delta\Delta\mu_{g-CT}$ for AN=CD and the smallest for AC=CD. On the other hand, the presence of a very weak acceptor substituent in aN=ND results in the smallest polarity of charge-transfer state among all the considered compounds.

Two-photon absorption spectra

Theoretically determined values of TPA cross sections (δ) to the CT state are presented in Table 5. The calculations were performed using three different functionals and also using the HF wavefunction. The latter approach gives the smallest values of the TPA cross sections of all the theoretical models employed. The CAM-B3LYP values of δ are much larger than the HF values but are still much smaller than those calculated using asymptotically incorrect functionals, namely the B3LYP and the BLYP. In general, the values of δ are significantly larger in the presence of a polar environment (see Table 5). The increase can be as large as 100%. Moreover, and not surprisingly, δ is quite sensitive to the nature of the D/A substituents [24]. For three pairs of different substituents, the following relation holds both for isolated molecules even when solvent effects are taken into account:

$$\delta_{AN=ND} > \delta_{AN=Nd} = \delta_{aN=ND}$$

The presence of two strong D/A substituents significantly enhances the values of the TPA cross section. Any change of one of the substituents to a weaker acceptor/donor leads to a decrease in δ value by a factor of two. A larger decrease in δ can be induced by weakening the electron accepting substituents. This was confirmed by Antonov et al. [24, 25], who observed the largest TPA intensity for the AN=ND compound and the smallest for aN=ND. Qualitatively, this result can be explained based on the energy differences between the charge transfer state and the ground state, which, for aN=ND and AN=Nd, is larger than in the case of AN=ND. Based on the data presented in Tables 5 and 6, we can conclude that a carbon–carbon π-bridge is more optimal as far as maximisation of δ is concerned. The value of δ calculated for AC=CD is almost two times larger than the value found for AN=ND. On the other hand, the presence of a heteronuclear π-bridge in the system might lead to either an increase or decrease in δ value. To relate the TPA properties of the investigated systems to their electronic structure, the so-called TSM, which accounts for two electronic states only—the ground (g) and the low-lying charge-transfer excited state (CT), was employed [46]:

$$\langle \delta_{gCT} \rangle \approx \left\langle \delta_{gCT}^{zz} \right\rangle = \frac{16}{5} S_{zz}^2 = \frac{16}{5} \cdot \frac{\langle g|r_z|CT\rangle^2 (\Delta\mu)^2}{\omega_{gCT}^2} \qquad (6)$$

where ⟨g|r|CT⟩ is the electric dipole transition moment, Δμ stands for the dipole moment difference, and ω_{gCT} corresponds to the transition energy. The equation is true for systems with a distinct direction of charge transfer (here, the *z*-axis). The values of the TPA cross-sections computed according to Eq. 6 are presented in Tables 6 and 7. As we

Table 8 Measured [18, 19] and calculated TPA cross-section using Eq. 7. The value of Γ_F was taken from [18, 19]. All values are in GM (1 GM= 10^{-50} cm^4 s photon^{-1} molecule^{-1})

	$\sigma^{(2)}_{DMSO}$ exp	$\sigma^{(2)}_{gas\,phase}$				$\sigma^{(2)}_{DMSO}$			
		HF	B3LYP	BLYP	CAM-B3LYP	HF	B3LYP	BLYP	CAM-B3LYP
AC=CD	191	45.9	208.8	141.5	156.4	–	313.7	194.2	253.4
AN=CD	76	22.7	159.7	129.6	76.7	44.8	247.3	197.6	141.9
AC=ND	133	57.2	208.2	130.9	151.5	84.2	311.9	175.0	240.8
AN=ND	178	40.0	132.2	111.3	88.3	88.2	219.3	165.2	150.4
AN=Nd	118	24.2	95.3	91.6	56.0	42.4	143.1	128.5	86.7
aN=ND	77	24.7	48.4	38.5	48.3	34.4	65.1	61.8	65.1

Table 9 Results of calculations [using 6–31+G(d) basis set] of molecular hyperpolarisabilities (β) for geometries optimised at the B3LYP/6–311++G(d,p) level of theory. All values are in atomic units (a.u.)

β	Gas phase					DMSO				
	MP2	HF	BLYP	B3LYP	CAM-B3LYP	MP2	HF	BLYP	B3LYP	CAM-B3LYP
AC=CD	10,052	5,115	23,805	17,610	10,006	40,849	18,184	129,226	107,367	14,277
AN=CD	6,526	3,051	14,417	9,375	5,787	21,267	8,808	100,316	51,941	7,859
AC=ND	7,319	4,033	28,340	19,110	8,648	22,334	10,977	148,264	108,632	13,014
AN=ND	10,329	4,944	16,954	13,230	8,634	43,934	18,051	91,026	72,509	13,102
AN=Nd	6,788	3,456	11,470	8,845	5,866	40,878	17,559	74,345	60,782	8,211
aN=ND	8,052	3,890	7,913	7,424	6,114	27,285	11,913	33,176	28,799	7,623

can see, the TSM overestimates TPA absorption cross section values. The ratio of the values calculated based on the response functions formalism and using the two-level model does not exceed 1.5. Thus, the predictions of the TSM can be considered as satisfactory. The ordering is also predicted correctly with the exception of AC=CD and AC=ND compounds, for which the exact values calculated using response functions differ only insignificantly. In order to compare the calculated values of the TPA cross-sections with those determined experimentally ($\sigma^{(2)}$), we used the following relation [57]:

$$\sigma_{OF}^{(2)} = \frac{8}{c} \cdot \frac{\pi^2 \alpha \, a_0^5 \omega^2}{\Gamma_F} \langle \delta \rangle \tag{7}$$

where α is a fine structure constant, ω is the energy of the exciting photon (in the case of the TPA absorption process, one-half of the excitation energy), c is the velocity of light in vacuum, Γ_F is the broadening of the final state (F) due to its finite lifetime. The data presented in Table 8 can be compared directly to experimental values published by Antonov et al. [24]. In all simulations, a constant value of Γ_F equal to 0.25 eV was assumed. Firstly, we see that the solvent substantially enhances the values of the TPA cross-section. Secondly, which is even more important for critical assessment of the applied models, we see that the best agreement with experimental values is achieved for the BLYP and the CAM-B3LYP functionals. The average differences between experimental and theoretical σ values are 58, 25, 88 and 28 GM, for the HF, BLYP, B3LYP and CAM-B3LYP models, respectively.

The values of calculated two-photon absorptivities are in good agreement with values reported by other authors [20, 58]. Any differences may be attributed to different values of Γ.

First hyperpolarisability

Table 9 presents the results of calculations of molecular hyperpolarisabilities (β) for all investigated compounds. All applied theoretical methods can be ordered according to the absolute values of β:

$$\beta_{\mathrm{BLYP}} > \beta_{\mathrm{B3LYP}} > \beta_{\mathrm{MP2}} > \beta_{\mathrm{CAMB3LYP}} > \beta_{\mathrm{HF}}$$

Traditional exchange-correlation functionals give values of β that are too large in comparison to MP2 values, which we use here as a reference. In the case of numerous organic systems, the MP2 method tends to slightly overestimate the values of β and γ (second-order hyperpolarisability) although it usually provides a very reliable estimate of the NLO properties of molecules [21, 59, 60]. Interestingly, the CAM-B3LYP functional predicts the values of hyperpolarisabilities to be slightly lower than those predicted by the MP2 method. Moreover, if we consider the molecules of different π-bridges (AC=CD, AN=ND, AC=ND, AN=CD), the ordering of β values predicted by the two methods is slightly different. Despite the insignificant discrepancies between CAM-B3LYP and MP2 data, what follows below uses the former to discuss the relationship between the electronic structure of the studied systems and their NLO properties. The ordering at the MP2 level of theory is predicted to be:

$$\beta_{MP2}^{gas\,phase} AN = ND \rangle \beta_{MP2}^{gas\,phase} AC = CD \rangle$$

$$\beta_{MP2}^{gas\,phase} AC = ND \rangle \beta_{MP2}^{gas\,phase} AN = CD$$

Table 10 Comparison of the β values calculated using finite-field (FF) approach and the two-state model (TSM, see Eq. 8). In the latter case, the excited state corresponds to the lowest-lying charge-transfer state

	β_{zzz}	
	TSM	FF
AC=CD	29,296	17,158
AN=CD	14,946	10,033
AC=ND	23,554	14,411
AN=ND	21,632	14,855
AN=Nd	14,294	10,071
aN=ND	−14,923	−10,544

As we see, traditional functionals overestimate the value of β by a factor of between two and five.

Changing the environment from the gas-phase to DMSO leads to a significant increase in hyperpolarisability, with threefold and fourfold increases in the case of AN=CD and AC=ND, and AC=CD and AN=ND, respectively.

In order to analyse first-order hyperpolarisability in terms of electronic excited states, the two-level model proposed by Oudar and Chemla was employed [26]:

$$\beta^{TSM}(0;0,0) \approx \beta^{TSM}_{zzz}(0;0,0) = 6\frac{\langle g|r_z|CT\rangle^2 \cdot \Delta\mu}{\left(\omega_{gCT}\right)^2} \qquad (8)$$

where $\langle g|r_z|CT\rangle$ is the transition moment, Δμ stands for the dipole moment difference between the low-lying CT state and the ground state and $\hbar\omega_{gCT}$ is the excitation energy to the CT state. A comparison of exact (for a given level of theory) and approximate (calculated according to Eq. 8) hyperpolarisability is presented in Table 10. Since the molecules were oriented in such a way that the dipole moment vector was parallel to the Cartesian *z*-axis it is not surprising that the dominant tensor element is β_{zzz}. The truncation of summation over electronic excited states leads to slightly larger values of β, but the ratio $\left(\frac{\beta^{TSM}_{zzz}}{\beta^{FF}_{zzz}}\right)$ does not exceed 1.7. This clearly indicates that the low-lying electronic excited CT state is by far the most dominant over others in the spectrum. The TSM thus predicts the ordering of compounds according to β quite satisfactorily.

Conclusions

This study presented the linear and NLO properties of selected azobenzene, stilben and benzilideneaniline derivatives, focussing on both resonant and nonresonant hyperpolarisabilities. Theoretical analysis of the electronic spectra showed that the most intense transitions to the charge-transfer state were observed for azobenzen derivatives, while the less intense oscillator strengths were found for benzilideneaniline derivatives. In general, the results of theoretical calculations of spectroscopic properties agree well with the available experimental data. As far as molecular resonant and non-resonant hyperpolarisabilities are concerned, the AC=CD system exhibited maximal values among all the considered molecules. Thus, stilben derivatives seem to be the most appropriate systems for NLO applications. On the other hand, benzilideneaniline derivatives exhibit larger NLO responses than azobenzene derivatives. What can also be observed is that nonplanarity of the π-backbone leads to molecular hyperpolarisabilities several orders of magnitude smaller than in the case of planar structures. The analysis of NLO response in terms of excited states shows that the low-lying charge-transfer state is essential for the values of the amplitudes of molecular resonant and non-resonant hyperpolarisabilities.

An important part of the present study was the testing of various exchange-correlation functionals commonly used for predictions of NLO properties. In particular, the recently proposed asymptotically corrected LC-BLYP and CAM-B3LYP functionals were employed. The results showed that, for isolated molecules, CAM-B3LYP predicts the values of excitation energies much closer to CC2 data than the LC-BLYP functional. On the other hand, a comparison of theoretical and experimental one-photon absorption spectra shows that both CAM-B3LYP and LC-BLYP functionals overestimate the transition energy in vacuo in comparison with more accurate treatments like CC2. The performance of DFT in simulating TPA is quite good. Of the functionals employed, the BLYP and CAM-B3LYP models give two-photon cross-section values much closer to experimental values than the B3LYP potential.

Acknowledgements Computational grants from the Poznan Supercomputing and Networking Center (PCSS) and ACK CYFRONET AGH are acknowledged. The author thanks Dr. Żaneta Czyżnikowska for computing excited state dipole moments using the CC2 approach.

References

1. Skotheim TJ (1986) Handbook of conducting polymers. Dekker, New York
2. Chemla DS, Zyss J (1987) Nonlinear optical properties of organic molecules and crystals. Academic, New York
3. Prasad PN, Williams DJ (1991) Introduction to nonlinear optical effects in molecules and polymers. Wiley, New York
4. Nalwa HS, Siezo M (1994) Nonlinear optics of organic molecules and polymers. CRC, Boco Raton
5. Zyss J (1994) Molecular nonlinear optics: materials, physics and devices. Academic, New York
6. Dalton LR (2001) Nonlinear optical polymeric materials: from chromophore design to commercial applications. Advances in polymer science, vol 158. Springer, Heidelberg
7. Dalton LR (2001) The role of nonlinear optical devices in the optical communications age. Kluwer, Dordrecht
8. Marde SRR, Perry JW (1994) Science 263:1706–1707
9. Denning RG (1995) J Mater Chem 5:365–378
10. Goonesekera A, Ducharme S (1999) J Appl Phys 85:6506
11. Stahelin M, Burland DM, Rice JE (1992) Chem Phys Lett 191:245–250
12. De Boni L, Piovesan E, Misoguti L, Zilio SC, Mendonca CR (2007) J Phys Chem A 111:6222–6224
13. Oliveira SL, Correa DS, Misoguti L, Constantino CJL, Aroca RF, Zilio SC, Mendonca CR (2005) Adv Mater 17:1890–1893
14. De Boni L, Misoguti L, Zilio SC, Mendonca CR (2005) Chem Phys Chem 6:1121–1125
15. De Boni L, Constantino CJL, Misoguti L, Aroca RF, Zilio SC, Mendonca CR (2003) Chem Phys Lett 371:744–749
16. van Walree CA, Franssen O, Marsman AW, Flipse MC, Jenneskens LW (1997) J Chem Soc Perkin Trans 2:799–807
17. van Walree CA, Marsman AW, Flipse MC, Jenneskens LW, Smeets WJJ, Spek AL (1997) J Chem Soc Perkin Trans 2:809–819

18. Baev A, Prasad PN, Samoc M (2005) J Chem Phys 122:224309
19. Chandra Jha P, Anusooya Pati Y, Ramasesha S (2005) Mol Phys 14:1859–1873
20. Day PN, Nguyen KA, Pachter R (2006) J Chem Phys 125:094103
21. Suponitsky KY, Tafur S, Masunov AE (2008) J Chem Phys 129:044109
22. Champagne B (1996) Chem Phys Lett 261:57–65
23. Jacquemin D, André J, Perpéte B (2004) J Chem Phys 121:4389–4396
24. Antonov L, Kamada K, Ohta K, Kamounah FS (2003) Phys Chem Chem Phys 5:1193–1197
25. Ohta K, Antonov L, Yamada S, Kamada K (2007) J Chem Phys 127:084504–084515
26. Oudar JL, Chemla DS (1977) J Chem Phys 66:2664–2668
27. Kawata S, Kawata Y (2000) Chem Rev 100:1777–1788
28. Delaire JA, Nakatani K (2000) Chem Rev 100:1817–1846
29. Adamo C, Scuseria GE, Barone V (1999) J Chem Phys 111:2889–2899
30. Jamorski-Jödicke C, Lüthi HP (2002) J Chem Phys 117:4146–4156
31. Cavillot V, Champagne B (2002) Chem Phys Lett 354:449–457
32. Becke AD (1993) J Chem Phys 98:5648–5652
33. Perdew JP, Burke K, Ernzerhof M (1996) Phys Rev Lett 77:3865–3868
34. Yanai T, Tew DP, Handy NC (2004) Chem Phys Lett 393:51–57
35. Tawada Y, Tsuneda T, Yanagisawa S, Yanai T, Hirao K (2004) J Chem Phys 120:8425–8433
36. Peach MJG, Benfield P, Helgaker T, Tozer DJ (2008) J Chem Phys 128:044118
37. Yanai T, Harrison RJ, Handy NC (2005) Mol Phys 103:413–424
38. Peach MJG, Cohen AJ, Tozer DJ (2006) Phys Chem Chem Phys 8:4543–4549
39. Iikura H, Tsuneda T, Yanai T, Hirao K (2001) J Chem Phys 115:3540–3544
40. Frisch MJ, Trucks GW, Schlegel HB, Scuseria GE, Robb MA, Cheeseman JR, Montgomery JA Jr, Vreven T, Kudin KN, Burant JC, Millam JM, Iyengar SS, Tomasi J, Barone V, Mennucci B, Cossi M, Scalmani G, Rega N, Petersson GA, Nakatsuji H, Hada M, Ehara M, Toyota K, Fukuda R, Hasegawa J, Ishida M, Nakajima T, Honda Y, Kitao O, Nakai H, Klene M, Li X, Knox JE, Hratchian HP, Cross JB, Bakken V, Adamo C, Jaramillo J, Gomperts R, Stratmann RE, Yazyev O, Austin AJ, Cammi R, Pomelli C, Ochterski JW, Ayala PY, Morokuma K, Voth GA, Salvador P, Dannenberg JJ, Zakrzewski VG, Dapprich S, Daniels AD, Strain MC, Farkas O, Malick DK, Rabuck AD, Raghavachari K, Foresman JB, Ortiz JV, Cui Q, Baboul AG, Clifford S, Cioslowski J, Stefanov BB, Liu G, Liashenko A, Piskorz P, Komaromi I, Martin RL, Fox DJ, Keith T, Al-Laham MA, Peng CY, Nanayakkara A, Challacombe M, Gill PMW, Johnson B, Chen W, Wong MW, Gonzalez C, Pople JA (2004) Gaussian 03, revision C.02. Gaussian, Wallingford CT
41. DALTON (2005) A molecular electronic structure program, Release 2.0 see http://www.kjemi.uio.no/software/dalton/dalton.html
42. Schmidt MW, Baldridge KK, Boatz JA, Elbert St, Gordon MS, Jensen JH, Koseki S, Matsunaga N, Nguyen KA, Su S, Windus TL, Dupuis M, Montgomery JA Jr (1993) The general atomic and molecular electronic structure system. J Comput Chem 14:1347–1363
43. Hättig C, Hald K (2002) Phys Chem Chem Phys 4:2111–2118
44. Hättig C, Köhn A (2002) J Chem Phys 117:6939–6951
45. Fliegl H, Köhn A, Hättig C, Ahlrichs R (2003) J Am Chem Soc 125:9821–9827
46. Zaleśny R, Bartkowiak W, Styrcz S, Leszczynski J (2002) J Phys Chem A 106:4032–4037
47. Krawczyk P, Kaczmarek A, Zaleśny R, Matczyszyn K, Bartkowiak W, Ziółkowski M, Cysewski P (2009) J Mol Model 15:581–590
48. Zaleśny R, Matczyszyn K, Kaczmarek A, Bartkowiak W, Cysewski P (2007) J Mol Model 13:785–791
49. Chen PC, Chiech YC (2003) Theochem 624:191–200
50. Rau H (1973) Angew Chem Int Ed Engl 12:224–235
51. Jacquemin D, Bouhy M, Perpéte EA (2006) J Chem Phys 124:204321
52. Jacquemin D, Preat J, Wahtelet V, Fontaine M, Perpéte EA (2005) J Am Chem Soc 128:2072–2083
53. Peach MJG, Helgaker T, Sałek P, Keal TW, Lutnaes OB, Tozer DJ, Handy NC (2006) Phys Chem Chem Phys 8:558–562
54. Jacquemin D, Perpéte EA, Scalmani G, Frisch MJ, Kobayashi R, Adamo C (2008) J Chem Phys 126:144105
55. Jacquemin, Perpéte EA, Scuseria GE, Ciofini I, Adamo C (2008) Chem Phys Lett 465:226–229
56. Liptay W (1974) In: Lim EC (ed) Excited states, vol 1. Academic, New York, p 129
57. Ch JP, Wang Y, Ågren H (2008) Chem Phys Chem 9:111–116
58. Day PN, Nguyen KA, Pachter R (2005) J Phys Chem B 109:1803–1814
59. Zaleśny R, Wójcik G, Mossakowska I, Bartkowiak W, Avramopoulos A, Papadopoulos MG (2009) Theochem 907:46–50
60. Medved M, Noga J, Jacquemin D, Assfeld X, Perpéte EA (2007) Theochem 821:160–165